IEEE Access
Multidisciplinary ⋮ Rapid Review ⋮ Open Access Journal

Received 24 June 2023, accepted 14 July 2023, date of publication 28 July 2023, date of current version 8 August 2023.

Digital Object Identifier 10.1109/ACCESS.2023.3299873

RESEARCH ARTICLE

Framework for Personalizing Wearable Devices Using Real-Time Physiological Measures

PRAKYATH KANTHARAJU[1], (Member, IEEE), SAI SIDDARTH VAKACHERLA[1], MICHAEL JACOBSON[1], (Member, IEEE), HYEONGKEUN JEONG[1], (Member, IEEE), MEET NIKUNJ MEVADA[1], XINGYUAN ZHOU[2], (Member, IEEE), MATTHEW J. MAJOR[3,4,5], AND MYUNGHEE KIM[1], (Member, IEEE)

[1]Department of Mechanical and Industrial Engineering, University of Illinois Chicago, Chicago, IL 60607, USA
[2]Department of Electrical and Computer Engineering, University of Illinois Chicago, Chicago, IL 60607, USA
[3]Research Health Scientist, Jesse Brown VA Medical Center, Chicago, IL 60607, USA
[4]Department of Physical Medicine and Rehabilitation, Feinberg School of Medicine, Northwestern University, Chicago, IL 60611, USA
[5]Department of Biomedical Engineering, McCormick School of Engineering, Northwestern University, Evanston, IL 60208, USA

Corresponding author: Myunghee Kim (myheekim@uic.edu)

This work was supported in part by the National Science Foundation (NSF) and the National Institute for Occupational Safety and Health (NIOSH) under Grant SES-2024863, in part by the United States (U.S.) Army Research Laboratory under Contract W911NF-21-2-0230, and in part by the U.S. Department of Veterans Affairs Rehabilitation Research and Development Service through Small Projects in Rehabilitation Research (SPiRE) Award under Grant I21RX004077.

This work involved human subjects or animals in its research. Approval of all ethical and experimental procedures and protocols was granted by the UIC IRB under Application Nos. UIC 2019-0087 and UIC 2020-0563.

ABSTRACT Personalizing wearable robots by incorporating user physiological feedback can improve energy efficiency and comfort. However, many current personalization methods are specific to a particular device and often require reprogramming, making them less accessible. In this study, we present an open-source, device-independent personalization framework that allows for human-in-the-loop optimization. This modular framework includes cost functions and optimization algorithms that use a physiological response to optimize wearable robot parameters. We tested this framework in three case studies involving diverse subjects and wearable robots. The first case study focused on personalizing an ankle-foot prosthesis using indirect calorimetry feedback. This resulted in a 5.3% and 18.1% reduction in metabolic cost for walking for two individuals with transtibial amputation, compared to the weight-based assistance. The second case study personalized a robotic ankle exoskeleton for three different walking speeds using indirect calorimetry feedback for two subjects. The metabolic cost was reduced by 1%, 2%, and 5.8% for one subject and by 20.8%, 1.9%, and 19% for the other subject, compared to a generic assistance condition for increasing speeds. The third case study personalized gait parameters, specifically step frequency, using an electrocardiogram (ECG)-based cost function along with an optimization algorithm variant, resulting in a 43% reduction in optimization time for one non-disabled subject. These case studies suggest that our personalization framework can effectively personalize wearable robot parameters and potentially enhance assistance benefits.

INDEX TERMS Wearable device, personalization, human-in-the-loop optimization, exoskeleton, prosthesis, metabolic cost, electrocardiogram.

I. INTRODUCTION

A wearable robot is a promising technology for assistance [1], [2], [3], [4], [5], [6], [7] and rehabilitation [1], [2], [8], [9]; however, the practical design of the device has been challenged [6], [10], [11]. One main challenge is high inter-subject variability, such as biomechanics [12], [13], [14], which results in various assistance outcomes [10]. Recent studies addressed inter-subject variability by personalizing assistance methods to meet each user's needs. One of the

The associate editor coordinating the review of this manuscript and approving it for publication was Tao Liu.

successful personalization methods is a data-driven approach known as Human-in-the-loop (HIL) optimization [1], [4], [15], [16], [17], [18], [19]. HIL optimization often uses a physiological [1], [3], [16], [17] or kinematic measure [2], [14] to increase the effectiveness of wearable robots in decreasing user's physical effort during walking [2], [3], [5], [16], and various activities [1], [4], [20].

Several HIL optimization methods have been proposed focusing on the optimization algorithm. Felt et al. [19] presented one of the early implementations of the personalization method, called body-in-the-loop optimization. In that study, directly minimizing energy consumption using a physiological outcome, namely respiratory measure, could allow users to converge onto an energy-efficient cadence. For the optimization method, the authors used a gradient descent search algorithm. Kim et al. [17] used a non-parametric, sample-efficient, and noise-tolerant method, Bayesian optimization (BO), to identify an energy-efficient step frequency. Using BO, the HIL optimization identified the optimal parameters twice as fast as the method proposed by Felt. et al. [19]. Then, the HIL BO method was used to identify an optimal parameter in a soft exosuit [16], which reduced the metabolic cost of walking by 17% compared to not wearing the exoskeleton. Zhang et al. [3] used a genetic algorithm, covariance matrix adaptation evolution strategy (CMA-ES), to personalize ankle exoskeleton assistance, which reduced the metabolic cost of walking by 24%, compared to the zero-torque condition. This HIL optimization approach was further expanded to other activities of daily living, such as running [4] and walking at various speeds [20]. However, the genetic algorithm-based parameter optimization takes a substantially long time to identify the optimal parameter [3], [20], [21]. Considering the practical need for minimizing in-vivo experimental time, the HIL Bayesian optimization [16], [17], [22], [23] might be applicable to various populations and clinical groups, including individuals with reduced physical strength and physically intensive activities, due to its sample efficiency and ability to quickly identify an optimal condition.

Researchers have investigated faster cost function estimation to reduce the optimization time and improve user comfort. One of the methods is reducing the steady-state metabolic cost using a phase plane estimation (PPE) instead of the time domain [22] method. This data-driven PPE method determined the steady-state metabolic cost twice as fast than the conventional method [22] using Gaussian mixture regression [24], [25], [26]. The effectiveness of this PPE method in a cost function was tested by HIL Bayesian exoskeleton parameter optimization during a squat [1]. With the new estimation method, two optimal parameters were found in 15 min, which helped to reduce steady-state metabolic cost by 20% compared to the no-device condition [1].

Other alternative cost functions have been developed. Jacobson et al. [2] showed that a symmetric function in the form of force time integral could be used as a proxy measure in place of the metabolic cost for the individuals with simulated amputation. The new cost function was used to identify personalized assistance in an ankle-foot prosthesis during walking. Han et al. [27] and Jeong et al. [28] showed that muscle activity-based measures could be used in HIL optimization. Slade et al. [5] used device measurements and a data-driven estimation process to personalize exoskeletons in the outdoor environment. Ingraham et al. [29] demonstrated that optimal assistance of an exoskeleton could be inferred using subjective feedback and user preference. These different cost functions could help optimize assistance in outdoor and more dynamic environments.

In addition to kinematic and calorimetric measures, several electrocardiogram (ECG) measures have shown a correlation with exercise intensity [30], [31], [32] with a less noisy and faster response than metabolic rate [33]. Therefore, ECG-based optimizations may result in faster optimizations compared to the use of the indirect calorimetric measure. In this toolbox, we incorporated the root mean square of successive R-R (peak in the ECG data) interval differences (RMSSD), a widely used ECG feature, as the candidate cost function [34]. RMSSD is a time series function that is relatively easier to compute than the non-linear or frequency-based cost functions [35]. This function correlates with exercise intensity and could be a valid indicator of metabolic cost [31], [35], [36], [37].

The progress in personalization has been significant; however, various optimization [1], [3], [5], [16], [20], and cost estimation methods [5], [22], [38], [39] typically involve custom optimization setup. In addition, a new system would require significant tuning and reprogramming of the communication system between the optimization outcomes and wearable robots [1], [17]. This variability and tuning increase the barrier to entry for exoskeleton (and prosthetic) personalization. We propose a HIL optimization framework with a communication protocol - lab-streaming layer (LSL).[1] LSL, is a TCP-based network communication protocol that has been implemented in various physiological sensors as it allows near-real-time access to time series information and synchronization. This setup will be modular, capable of configuring the cost function and optimization methodologies.

To demonstrate the capabilities of the proposed framework, we performed a proof-of-concept study of the framework in three different case studies with varying cost function (metabolic cost, ECG, foot pressure), varying subject populations (individuals with below knee amputation, Non-disabled individuals) and varying assistance devices (ankle-foot prosthesis, ankle exoskeleton, and walking step frequency). The manuscript is divided into three different sections. In the first section, we introduce the framework in detail by explaining different modules: human-machine system, cost function estimation, and the Bayesian optimization module. We validated the framework via three case studies, (1) HIL ankle-foot

[1] https://github.com/sccn/labstreaminglayer

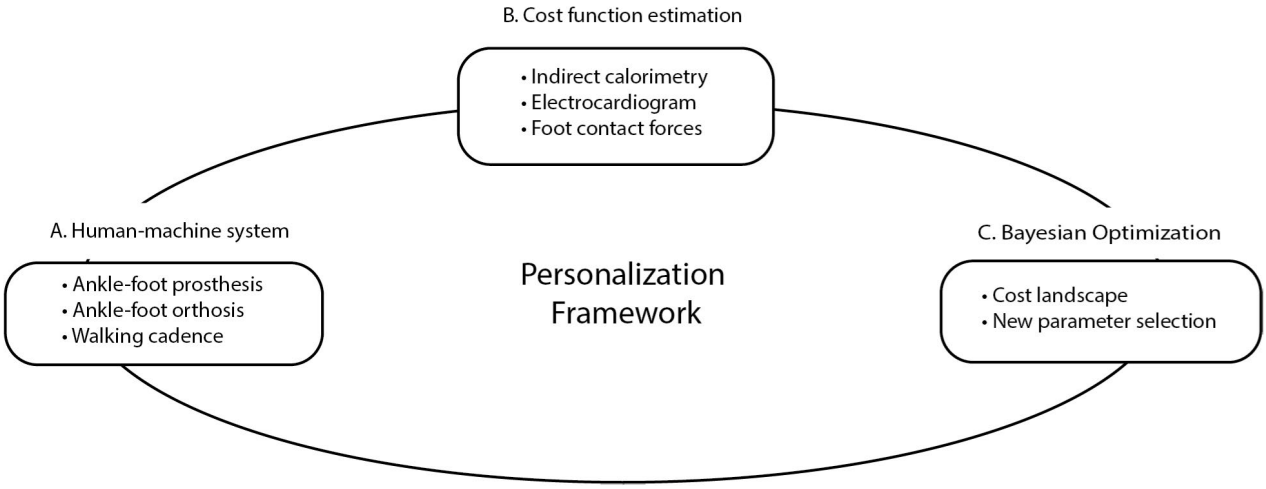

FIGURE 1. Overview of the personalization framework: The figure presents an overview of the personalization framework. The framework is divided into three parts: (A) Human-machine system: As an example, we demonstrated three different systems: ankle-foot prosthesis - walking with individuals with simulated amputation, persons with below knee amputation, ankle-Foot orthosis - walking and squatting with non-disabled individuals, and auditory command - step frequency for non-disabled, (B) Cost function estimation: we predicted cost using indirect calorimetry, electrocardiogram (ECG), and foot contact force measures to evaluate the effectiveness of the personalized assistance, and (C) Bayesian Optimization: assistance parameters were optimized by generating the cost landscape (Gaussian process) and selecting the next parameter (Acquisition function).

prosthesis parameter optimization with individuals with transtibial amputation; (2) HIL robotic exoskeleton parameter optimization for various walking speeds; (3) HIL gait parameter optimization using a different cost function and Bayesian optimization variants. Finally, this framework's potential impact and results from the case studies are discussed. All the data collection code and setup are provided in the following GitHub repository: https://github.com/UICRRL/HIL_toolkit.

II. FRAMEWORK

The framework is comprised of three components: A) human-machine system, B) Cost function estimation - to predict user outcomes given assistance, and C) Bayesian optimization - to evaluate cost landscape given assistance and measured costs, and then select the next parameter (Fig. 1). In this section, we provide a comprehensive explanation of these components.

A. HUMAN-MACHINE SYSTEM

The first module of this framework is the human-machine system. In particular, we aim to optimize the machine parameter to meet each human's needs. The machine can be a wearable robot (e.g., robotic ankle-foot prosthesis or robotic ankle-foot orthosis) or commands from a device (e.g., auditory cues). The machine provides assistance, and the human conducts an activity given assistance while interacting with the machine. In this framework, we personalized parameters for three human-machine systems.

1) ROBOTIC ANKLE-FOOT PROSTHESIS (AFP) EMULATOR

We used a two-degree-of-freedom robotic ankle-foot prosthesis with an active plantarflexion and in/eversion [40]. This AFP comprises an aluminum frame, two toes, and a compliant heel. The compliant heel uses a heel fiberglass spring (Gordon Composites, Montrose, CO). The rotation of each shaft-toe assembly resembles the natural dorsiflexion and plantarflexion of an anatomical ankle joint. Two encoders mounted to the frame measured the angle for each toe's axis, and a load cell was used to measure the actual torque observed. This AFP provides assistance by providing ankle torque during the stance phase of the gait cycle. The level of assistance is determined using a predefined ankle-torque curve parameterized with stiffness parameters.

In our prior work, we personalized this parameter iteratively using a foot pressure sensor [2] or respiratory measures [23] for individuals with simulated amputation. This study further developed a framework structure and tested it on two individuals with transtibial amputation (Case Study 1).

2) ROBOTIC ANKLE-FOOT ORTHOSIS (AFO)

The one-degree-of-freedom robotic ankle exoskeleton (AFO) (Humotech, Pittsburg, PA) was used as another machine system interacting with a human [7]. The exoskeleton provides assistance based on a predefined, parameterized ankle-torque curve. The parameter was personalized here through a human-in-the-loop optimization algorithm for a squatting activity using an ankle exoskeleton [1] similar to [7]. Based on this method, we developed a framework and tested it for walking assistance (Case Study 2).

3) WALKING CADENCE

Walking cadence optimization has been used to evaluate human-in-the-loop optimization methods [17], [19]. We also used an audible metronome tone and a human system to test

the personalization algorithm performance using a new cost function based on heart rate and acquisition functions. Details of the optimization can be found in the (Case Study 3).

B. COST FUNCTION ESTIMATION

The user outcome given assistance is recorded and used to determine the best assistance for the user. The cost function estimation is the module to determine the user's physical effort using physiological signals [41]. In this framework example, three signals have been used to quantify the effect of the assistance.

1) INDIRECT CALORIMETRY

This sensor information was used to estimate the conventional metabolic cost [22], [39], [42]. We measured the breath-by-breath VO2 and VCO2 using a respiratory measure (K5, Cosmed, Italy). The metabolic rate was calculated using VO2 and VCO2 based on the Brockway equation [43]. The sensor was calibrated before every session, and respiratory data were monitored using the COSMED Omnia (data collection application and real-time SDK). The metabolic rate is transferred to LSL using a custom python script. Using this real-time metabolic rate, we estimated the steady-state metabolic cost using Phase plane estimation (PPE) and Instantaneous Cost Mapping (ICM).

a: PHASE PLANE ESTIMATION (PPE)

PPE is a fast, data-driven metabolic cost estimation method proposed in our previous work [22]. This method transforms the time-series metabolic rate to the phase plane. In this phase plane, the forward difference of the metabolic rate is mapped into the vertical axis, and the metabolic rate is described in the horizontal axis (Fig. 2.A). The steady-state metabolic cost estimate does not change over time; hence, it can be assumed that the steady-state metabolic cost is a point on the horizontal axis where the vertical axis value is zero. The Bayesian Gaussian mixture clustering [26], [44] was used to cluster the data in the phase plane and estimate each cluster's mean μ and covariance Σ. The Gaussian mixture means and covariance were used to estimate the steady state point on the X-axis, as shown in the equation below

$$\text{steady state} = \frac{\sum_k^K A_k}{\sum_k^K B_k}$$

where A and B are the regression coefficients for each cluster k given by $\Sigma_{x,y}/\Sigma_x$, and $\mu_y - A \cdot \mu_x$. This estimation is performed for each breath. Implementation details and comparisons are presented in [1] and [22]. The step-by-step algorithm is provided in the supplementary material (section 4.1).

b: INSTANTANEOUS COST MAPPING (ICM)

ICM is a commonly used estimation method for HIL optimization [3], [4], [16], [19], [20]. The metabolic rate and steady-state metabolic cost are modeled as a mono-exponential model. A discretized version of this method is presented as follows,

$$z(i+1) = \frac{\tau - dt(i)}{\tau} \cdot z(i) + \frac{dt(i)}{\tau} \cdot z^*$$

Here, $z(i)$ is the metabolic rate measured at the time (i), and z^* is the steady-state metabolic cost function that needs to be estimated. The $dt(i)$ is the time difference between the breath i and the next breath $i+1$, and τ is the time constant. We have initialized τ in this system as 42 based on the Selinger et al. [39] recommendation. However, this parameter needs to be changed based on the activity, as suggested by [4]. A detailed algorithm is presented in the supplementary material (section 4.2).

2) ELECTROCARDIOGRAM (ECG)

A recent study found that ECG information can be used to predict metabolic cost [41]. In this study, ECG was measured using a polar H10 chest strap (Kempele, Finland) and was filtered using a real-time filter [45]. The sampling rate of the ECG sensor was fixed at 130 Hz. Data is streamed over Bluetooth low-energy (BLE) protocol and captured by a custom python script which transfers it to LSL every 1 sec.

a: R-R (PEAK IN THE ECG DATA) INTERVAL DIFFERENCES

We used the root mean square of successive R-R interval differences (RMSSD) to estimate energy expenditure [41]. To calculate the RMSSD in real-time, we first filtered the ECG data using a 0.5 Hz high-pass 5th-order Butterworth filter and removed any linear drift. The R-R peaks were identified using the method proposed by Kalidas and Tamil [46]. The time intervals between R-R peaks were squared and averaged for a time range. The square root of the average was used as the cost function. We used the neurokit2 library [47] and the custom python-based data processing pipeline for real-time cost estimation. For this experiment, we used a 30s interval for R-R peaks identification and for cost calculations [48]. A detailed method is provided in the supplementary material (section 4.5).

3) FOOT CONTACT FORCES

In our prior work, we have shown that foot contact forces can be used to predict the energy expenditure of walking [2]. The contact forces were measured using F-scan foot pressure sensors (Tekscan, MI, USA). These sensors are placed over the left and right insole and calibrated using the F-scan step calibration method [2]. Both sensors have 25 sensels per square inch, and pressure information at each sensel is transferred using the USB communication protocol and accessed through Tekscan API at 120 Hz. In our previous implementation, the data was obtained using MATLAB, but in this framework, we have set up the acquisition using a custom python application to integrate this physiological measure into the proposed framework. This data is sent to LSL every 1 sec.

a: FOOT FORCE TIME INTEGRAL (FFTI)

FFTI estimates the metabolic cost of steady-state walking using gait asymmetry information [2]. For each left and right limb, we first calculated the foot contact force applied during walking and integrated it across the stance phase. This value was used to calculate the symmetric index (SI) [49]. The SI was used to determine the asymmetric cost and estimate the approximate metabolic cost (details are described in our previous study [2]). The detailed algorithm and step-by-step instructions are provided in supplementary section 4.3.

Algorithm 1 Bayesian Optimization

while Not converged **do**
  Measure cost (y_i) for parameter ($\mathbf{x}_i$)
  $y_i^* \leftarrow y_i + \epsilon,\ \epsilon \sim \mathcal{N}(o, \sigma_{noise})$ ▷ Gaussian Noise
  $\mathbb{D} \leftarrow y_i^*, x_i$
  Posterior function
  $\mu(\mathbf{x}_*) = k_n \cdot (K + \sigma_{noise}^2 \cdot \mathbb{I})^{-1} \cdot \mathbf{y}_{1|n}$ ▷ Mean of Gaussian Regression
  $\sigma(\mathbf{x}_*)^2 = K - k_n \cdot (K + \sigma_{noise}^2 \cdot \mathbb{I})^{-1} \cdot k_n^T$ ▷ standard deviation of Gaussian Regression
  Acquisition function
  $V_{\mathbf{x}_*} \leftarrow acq(\mu_{x_*}, \sigma_{x_*})$ ▷ Generate the value for acquisition function
  $x_{n+1} \leftarrow argmax(V_{\mathbf{x}})$ ▷ Selecting the parameter with the large value as next parameter
  Convergence criteria
  if time > experiment time ‖ $x_{n+1} == x_n == x_{n-1}$ **then**
    Converged
  else
    Not Converged
  end if
end while

C. BAYESIAN OPTIMIZATION

In this framework, BO is a module that optimizes parameters given various cost functions (Fig. 1B) and device parameters (Fig. 1A). BO is a semi-global, non-parametric, and noise-tolerant method [50], [51]. Typically, BO involves two sequential optimization steps; the first is the generation of the posterior distribution [35], [36], and the second is sampling the next optimization point using the acquisition function.

1) COST LANDSCAPE

We used the Gaussian process (GP) as the posterior function for its sample efficiency, non-parametric, and noise tolerance characteristics [52], [53]. This function uses the data and kernel functions to estimate the posterior function, with mean and covariance at each point in the sample space.

The construction of the posterior function's mean and covariance at each point (x_*) on the sample space can be found in Algorithm 1. Here, k_n is a vector obtained by applying the kernel function (k) on known data points x_n and sample space x_* in the form $k_n = k(x_n, x_*)$. K is the matrix obtained by applying kernel function (k) on the entire sample space (x_*) in the form $\mathrm{K} = \mathrm{k}(x_*, x_*)$. The σ_{noise} is the hyper-parameter tuned during the construction of the Gaussian process. The hyper-parameter training is detailed in the supplementary material (section 3).

We used the squared exponential (SE) kernel as a standard practice [1], [16]. It is easy to switch kernels depending on the application. Supplementary section 1 explains the kernel options and expected behavior for each kernel.

2) NEW PARAMETER SELECTION

The new parameter was typically selected using the mean and standard deviation of the posterior function [50] while balancing between exploration and exploitation. In this example, we mainly used Expectation Improvement (EI) [54], explained in the Acquisition function section in Algorithm 1. The μ_{x_*} and the σ_{x_*} are the mean and standard deviation of the posterior function (Gaussian process) at each point x_* in the sampling space. The f_{best} - best output observed with the sampling point is used to construct a matrix (V_{x_*}). The matrix calculation depends on the acquisition function (e.g., EI, Probability of improvement (PI), Upper Confidence Bounds (UCB) [54]). The sampling points corresponding to the maximum value are selected as the next points in the optimization loop (argmax (V_x) in the algorithm). Several other methods, such as noisy EI or Monte Carlo-based functions [55], [56], can be used depending on the application. In supplementary section 3, we provide a detailed explanation of regularly used acquisition functions and compare the performance of these acquisition functions for a standard optimization procedure.

III. CASE STUDIES

A. (CASE STUDY 1) ANKLE-FOOT PROSTHESIS (AFO) OPTIMIZATION

We tested the proposed HIL optimization framework to personalize AFP assistance for individuals with transtibial amputation (Fig. 2.1). The primary motivation of this case study was to test the feasibility of the proposed framework with various populations. We used the conventional metabolic cost-based optimization and validated the personalized assistance with a weight-based, generic condition and a prescribed prosthesis condition (Fig 2.2).

1) THE PERSONALIZATION FRAMEWORK

a: HUMAN-MACHINE SYSTEM (ROBOTIC AFP EMULATOR)

We used the AFP emulator described in Section II-A.1. The device could generate a maximum plantarflexion torque of 140Nm; however, we set the torque threshold at 120Nm, considering the safety of the subjects and the device. The control system was composed of two levels, low- and high-level controllers. The low-level controller tracked the desired torque using a proportional controller based on the torque error between desired and measured torques. The high-level

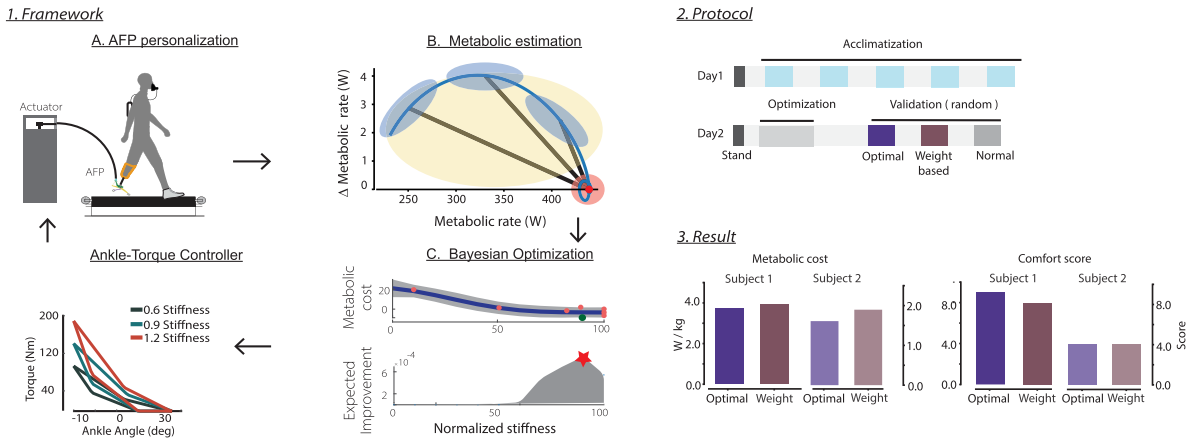

FIGURE 2. Ankle-foot prosthesis personalization: (1) the personalization of prosthesis using the framework, (2) the two-day protocol used to find personalized assistance parameters using the framework and validate the experimental results, and (3) the metabolic costs and the comfort scores for two participants during the validation conditions.

controller generated the desired ankle angle and torque curve using the stiffness parameter from the BO module.

b: COST FUNCTION (RESPIRATORY MEASURE)

We used the metabolic cost of walking using the respiratory measure using the PPE algorithm. We used 1.5 min data per each optimization condition.

c: BAYESIAN OPTIMIZATION

The BO module iteratively fitted the data to the GP landscape and then selected the next parameter using the EI. The parameter scale ranged from 0.5 to 1.4 N/deg for subject 1 and 0.5 and 1.5 N/deg for subject two for the study below. The range was selected based on the subject's weight, age, and height and kept constant throughout the experiment.

2) EXPERIMENTAL PROTOCOL

We tested the personalization method with two individuals with transtibial amputation (age: 38 and 59 yrs, prosthesis use: 17 and 23 years, weight: 95 and 60 kg, Height: 185 and 170 cm, male and female) using two days of experimental protocol (Fig. 2.2) (Protocol No: UIC IRB 2019-0087). We collected the respiratory measures and, additionally, user comfort with a comfort score adapted from the socket comfort score [57] [0-10, 10 is the most comfortable device for walking, and 0 is very uncomfortable].

On Day1, the robotic ankle-foot prosthesis end-effector was fitted to the participant by a certified prosthetist. Then, the subject was instructed to walk for five stiffness conditions for 5 min, composed of the control off condition (motion position constant) and four conditions with different assistance profiles. 5 min rest was given in between trials.

On Day2, two-minute initial conditions were performed to validate the attachment of the prosthesis. Then, the HIL optimization was conducted for 14 min. Following the optimization, the optimal, weight-based condition (sub 1: 0.8, sub 2: 0.6 [10% of body weight in kg] [2]) and their prescribed (customary) prosthesis were evaluated. 1:1 rest time was provided for all the conditions on Day1 and Day2.

3) RESULTS

The personalized assistance (optimal condition) was identified for subjects 1 and 2 in 6 and 7 optimization iteration, and optimization lasted for 620 and 720s, respectively. Personalization reduced metabolic costs by 5.6% and 18.1% for the optimal condition compared to the weight-based condition. For the prescribed prosthesis condition, Subject 1's steady state metabolic cost was 4.61 W $\cdot$ kg^{-1}, which was 23.5% higher than the optimal condition. Subject 2's metabolic cost was 1.40 W $\cdot$ kg^{-1}, which was 14% lower compared to the optimal condition. Subject 1 reported that robotic AFP was more comfortable compared to their prescribed prosthesis, with a comfort score of 9 and 8 for the optimal (personalized) and weight-based condition and 7 for their prescribed prosthesis. Subject 2 reported that both the weight-based and optimal assistance had the same comfort score of 4, while their prescribed prosthesis scored a 9. These comparisons between the weight based and the optimal condition show that our framework can be successfully applied to different populations, including clinical groups.

B. (CASE STUDY 2) SPEED-SPECIFIC PERSONALIZED ASSISTANCE

We tested the framework for various activity conditions in non-disabled individuals (Fig 3.1), in this case, speeds (1 m/s, 1.25 m/s, and 1.5 m/s), as we hypothesized that the personalized assistance would be different for different speeds; hence, the framework should work for various activities. We tested by comparing the user outcomes from the speed-specific, personalized assistance condition to the generic and optimal assistance identified at normal walking speed (Fig 3.2).

1) THE PERSONALIZATION FRAMEWORK

a: HUMAN-MACHINE SYSTEM (ROBOTIC AFO EMULATOR)

We used a 1-degree of freedom (DOF) and tethered ankle exoskeleton (Humotech, Pittsburg, PA). We divided the gait cycle into swing and stance phases. These stages were identified using the heel and toe switches. During the swing

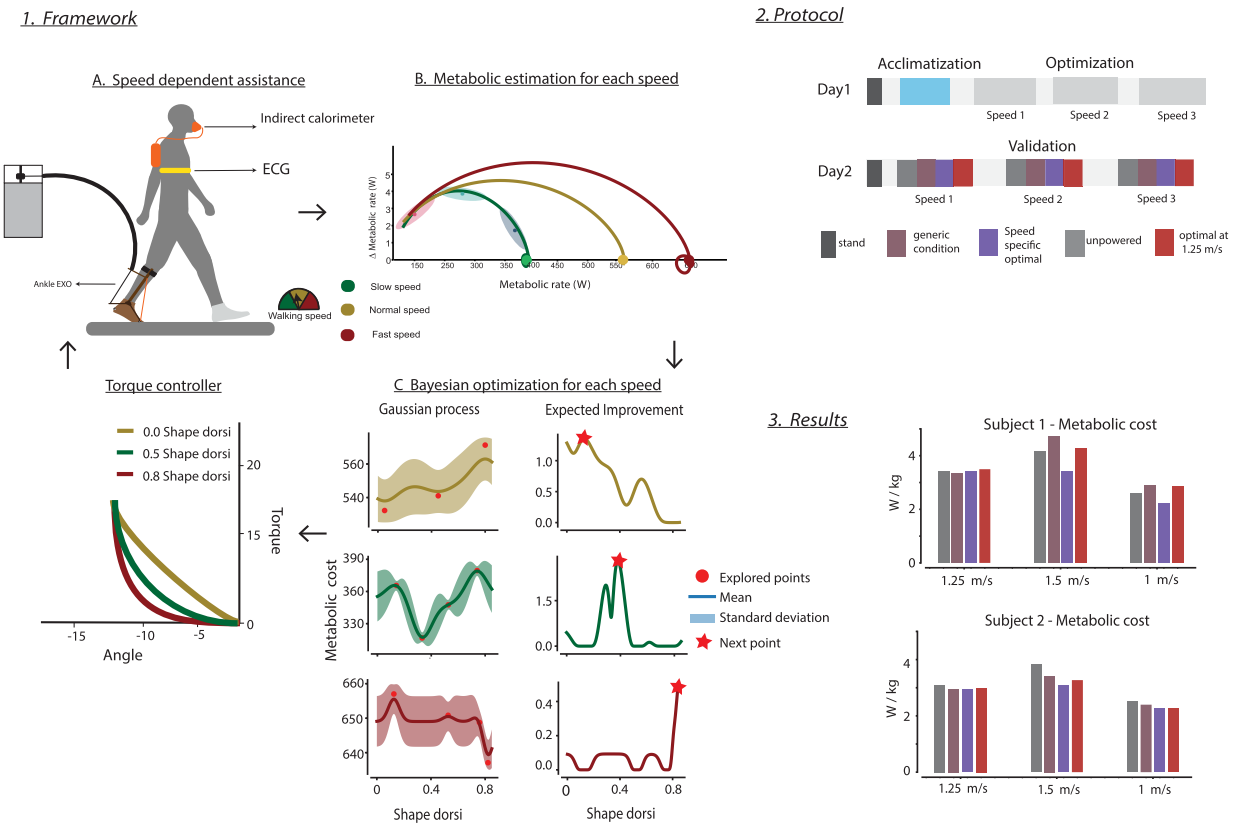

FIGURE 3. Ankle-foot exoskeleton personalization: (1) the personalization of orthosis for various speeds using the framework, (2) the two-day protocol used to personalize assistance using the proposed framework and validate the experiment, and (3) the metabolic cost observed during the validation condition for two subjects at 3 different speeds.

phase, we used a zero motor position controller so the subject could freely move to the next step. During the stance phase, the low-level controller conducted the torque control to track the desired torque. The high-level controller generated the desired torque curve based on the ankle angle and a shape-dorsi parameter (Fig 3.1, Torque controller) from the BO module.

b: COST FUNCTION (RESPIRATORY MEASURE)

We estimated the metabolic cost of walking at three different speeds using the PPE method and the respiratory measures.

c: BAYESIAN OPTIMIZATION

We performed optimization for each speed separately using metabolic cost as the cost function. To estimate the cost landscape, we used the GP with SE kernel, and for the acquisition function, we used EI. The shape-dorsi parameter range was 0-0.85 based on subject weight and device control range.

2) EXPERIMENTAL PROTOCOL

We used a two-day protocol to identify and validate the speed-specific optimal assistance (Fig. 2.2) with two subjects (Male, age: 27 and 19 years, weight 91 and 75 kg, Height 185 and 172 cm) (Protocol: UIC IRB 2020-0563). The walking speeds for low, medium, and high were 1 m/s, 1.25m/s, and 1.5 m/s, respectively.

On Day1, we performed an exoskeleton acclimatization trial at different speeds. During this trial, the subject walked under three different stiffness conditions for 2 min each for low, medium, and high-speed conditions (Order randomized for each subject). After each speed condition, a 7 min rest time was allocated for the subject. Following this acclimatization period, we performed the HIL optimization for each speed. Typically, the optimization process took 12 minutes, during which the optimizer selected consecutive parameters that indicated the best point. After each optimization, 7 min sitting rest time was provided to the subject.

On Day2, we validated the optimal parameters obtained on day one by comparing them with unpowered, generic conditions (fixed stiffness) and optimal conditions for normal speed. Each condition was further divided into three trials of 5 min for each speed. Between each speed trial, we provided 1 min of sitting rest time. After each condition, we provided 7 min of rest time. The order of each condition is randomized to reduce the learning effect.

3) RESULTS

The personalized assistance reduced steady-state metabolic cost for speed-specific optimal conditions compared to unpowered conditions. The metabolic costs were reduced by 5.8% and 18.8% for 1.5 m/s speed for subjects 1 and 2, respectively. Each participant reduced the metabolic cost of

walking by 1.8% and 2.0% for the speed-specific optimal condition compared to the unpowered condition at 1.25 m/s. They also reduced the cost by 0.5% and 20.8% for the 1m/s condition, respectively. On average, personalization took seven parameters and 820s, including the warm-up period.

Compared to generic and normal speed's optimal conditions, for each speed, we observed that speed-specific optimal conditions reduced metabolic costs for all other conditions. Detailed results are tabulated in the supplementary material (Section 5) and are also presented in Figure 3.3.

C. (CASE STUDY 3) STEP FREQUENCY OPTIMIZATION USING ECG

Step frequency optimization was conducted to demonstrate the compatibility of the framework for various options (Fig 4.1): a different human-machine system, a new cost function option, in this case, a new cost function using the physical effort estimate from ECG, and acquisition functions in BO. Specifically, we optimized walking cadence, a common practice to test a new algorithm [17], [19]. Step frequency or walking cadence is naturally optimized for a given walking speed to reduce energy consumption [58]. Previous studies have used this information to test different optimization schema and cost functions [17], [19]. Since this step frequency optimization was previously used to compare the different optimization schema [17], [19], this study can be used to directly compare the current optimization framework with published results and traditional energy measures such as metabolic cost.

1) THE PERSONALIZATION FRAMEWORK

a: HUMAN-MACHINE SYSTEM (AN AUDITORY CUE)

The subject was instructed to follow a metronome-set walking cadence, with a range set to ±15% of normal [17], [19]. We used a wireless speaker to deliver the metronome sound corresponding to the desired cadence.

For the ECG-based cost function with EI acquisition function, 0.88% difference compared to the preferred step frequency was identified as optimal within 4 iterations. Total optimization time, including a warm-up walk of 2 min, was 306s. For the ECG-based cost function with a Monte-Carlo sampling-based cost function (q-Noisy EI - qNEI), a 2% difference from the preferred step frequency was found to be optimum in 5 iterations. This optimization took 383s with the warm-up.

IV. DISCUSSION

We have developed a modular, personalization framework composed of a human-machine system, cost function estimation, and BO. The framework was tested with various A) human-machine systems, including individuals without disabilities and with transtibial amputation, robotic ankle-foot prosthesis and orthosis, and metronome-set gait; B) cost functions using respiratory measures and ECG; and C) BO with different acquisition functions (Table 1). For all scenarios, the personalized assistance reduced the metabolic cost compared to generic or control-off conditions. These results suggest that the proposed framework can be used to personalize assistance while accommodating diverse population-machine systems, cost functions, and BO variants. The framework application also presented its abilities in two different scenarios: assisted squatting activity with non-disabled and robotic AFO system (A), utilizing metabolic cost estimation (B) and a regular BO (C) [1]; and assisting walking with individuals who had a simulated amputation using robotic AFP (A), physical effort estimation using foot contact forces (B), and regular BO (C) [2]. In addition, our modular framework is lightweight, parallelized, and compatible with mobile computers, opening opportunities to perform optimization in outdoor settings.

A. CASE STUDY 1

Ankle-foot prosthesis personalization: When the framework was used to personalize assistance for individuals with transtibial amputation, the personalized assistance resulted in a maximum of 5.6% and 18.1% reductions for Subjects 1 and 2, respectively, compared to the generic condition.

Personalizing ankle-foot prostheses has been challenging [11], perhaps in part due to reduced strength for individuals with reduced mobilities. For these individuals, the extensive optimization time could induce fatigue and potentially subsequently lead to unsuccessful optimization. Our approach incorporates a rapid metabolic cost estimation method coupled with a sample-efficient Bayesian Optimization (BO) module for HIL optimization. This combination effectively trims the total optimization time down to a mere 12 minutes, which is a threefold speed increase compared to the conventional Human-In-The-Loop (HIL) optimization method that relies on Covariance matrix adaptation evolution strategy (CMA-ES) [11]. The faster optimization may have contributed to identifying better-personalized assistance as it could minimize long optimization-induced fatigue. To evaluate the efficacy, future work can include controlled human subject experiments with an increased number of participants to test the hypothesis that personalized assistance can maximize assistance benefits.

The robotic prosthesis' personalized and generic condition had higher metabolic costs than their prescribed, customary prosthesis for Subject 2. One possible reason could be the relatively larger size and weight of the AFP. The AFP was designed for a male subject with foot size 10, while the prescribed prosthesis was smaller, with size 9 for a female user. This difference between the prescribed prosthesis and the robotic AFP could have affected the participants' gait kinematics and led to changes in metabolic cost [59]. In addition, the participants with transtibial amputation had limited time to learn the robotic AFP use (1-2 hours), compared to their years of experience with their own prosthesis (Subject 1: 17 years, Subject 2: 23 years). Our recent study suggests that implementing a user training protocol can facilitate a faster

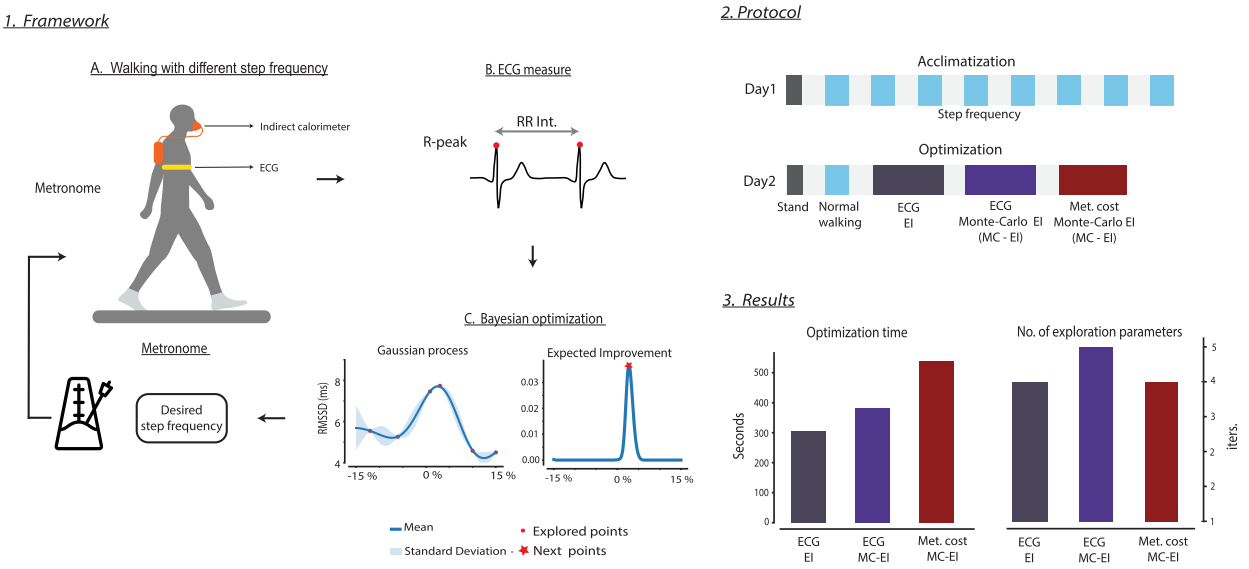

FIGURE 4. Step frequency optimization using respiratory measures and ECG with two acquisition functions: (1) the personalization method using the framework, focusing on ECG-based measures, (2) the two-day protocol performed to test the framework and validate the hypothesis, and (3) the optimization duration and the number of parameters explored for the personalization.

TABLE 1. Case studies using the framework.

	Case studies				
Activity	Walking	Walking	Walking	Squatting [1]	Walking [2]
A. Human-machine system	Ankle-foot prosthesis	Ankle-foot orthosis	Walking cadence	Ankle-foot orthosis	Ankle-foot prosthesis
	Individuals with transtibial amputation	Non-disabled	Non-disabled	Non-disabled	Simulated transtibial amputation
B. Cost estimation function	Metabolic cost	Metabolic cost	ECG	Metabolic cost	Foot contact forces
C. Bayesian Optimization	GP-EI	GP-EI	GP - EI, qNEI	GP-EI	GP-EI

learning process for device use, leading to a reduction in metabolic cost when walking with the wearable robot [40]. Future work should consider including such user guidance protocols in this framework to aid user adaptation to the wearable robot.

B. CASE STUDY 2

Speed-specific personalized assistance: The personalized assistance using this framework was found to reduce the metabolic cost by an average of 7.8% under speed-specific conditions compared to the generic assistance condition, indicating that this framework can be applied to various walking speeds. Furthermore, the optimization process took only 12 minutes, which is one-third of the time required by state-of-the-art methods for three different walking speeds. Recent studies have emphasized the importance of personalized assistance in natural settings, and these fast and adaptable optimization results could be useful for providing personalized assistance in the outdoor environment [5], [20].

C. CASE STUDY 3

Step frequency optimization: The personalization and modular framework successfully identified optimal frequency through the use of different cost function modules and BO modules. Especially when an ECG-based cost estimation module was used, the optimal step frequency was identified 43% faster than a respiratory-based cost estimation method, including PPE. Also, regardless of the BO module variants on the parameter selection method, the optimal point was found in 5 iterations. The ECG-based cost estimation also has additional advantages in terms of portability and wearer comfort, making it a desirable alternative to indirect calorimetry, which

relies on face masks, and it may help to optimize assistance in a natural setting.

The framework described in these case examples was developed using a BO. Although BO has been successfully used to personalize assistance in a short time [17], [60], it has a limitation in accounting for a time-varying response to prolonged exoskeleton usage [61], [62]. Future versions of this framework will include optimization algorithms to address time-varying dynamics, such as time-dependent BO algorithms [63]. A limitation of this proposed framework is that the machine in a human-machine system should operate based on a pre-determined parameter set, influencing human-machine system outcomes. For a wearable robot case, it is typically a parameterized trajectory and a relevant controller. To make this framework more accessible, an open and primitive controller will be added.

We have not conducted compatibility tests with all commercial exoskeletons and sensors. To mitigate this limitation, we designed our framework as a modular setup featuring customizable input and output configurations built upon an open-source protocol. We validated this setup using our custom-made prosthesis and exoskeletons [1], [64], [65], [66] and commercial exoskeleton [7]. For the sensor acquisition system, we conducted tests with three different physiological sensors. However, the potential exists for compatibility issues or errors with different devices. We have included an instruction manual, available for reference, in Supplementary Material section 9 (Instruction Manual). In our future work, we plan to broaden our framework's compatibility to encompass a wider range of sensors.

Another limitation associated with the proposed HIL toolkit is the necessity for hyperparameter tuning. Our toolkit relies on Bayesian optimization and a Gaussian process posterior function, which may exhibit sensitivity to kernel hyperparameters such as length scale and noise range. To address this, we have adopted stochastic gradient descent for hyperparameter optimization, employing the marginal log-likelihood as the cost function. Still, the task of adjusting the bounds and initial points of hyperparameters calls for a unique approach for each cost function and activity. In future work, we intend to use musculoskeletal simulations and existing knowledge to refine the hyperparameter tuning process more effectively.

The current user interface of our optimization framework is primarily designed for experienced engineers, which could potentially be a barrier for less experienced users or non-researchers. Recognizing this, we aim to make it more universally accessible. Future work can include developing a more user-friendly, perhaps even tablet-optimized, user interface. This will make the optimization tool more approachable and easier for a broader range of users.

V. CONCLUSION

In this study, we developed a personalization framework for wearable devices, consisting of a human-machine system, cost function estimation, and Bayesian optimization. The framework is designed to be both modular and versatile. By keeping the optimization algorithm constant while allowing for easy integration of different cost functions, this framework could help benchmark exoskeleton performance and personalize wearable robots for various populations. Additionally, the modular configuration of the framework allows for expansion and the ability to test multiple optimizations simultaneously in parallel. The results from case studies demonstrate that the framework is applicable for multiple populations, assistive devices, cost functions, and optimization setups. Overall, this framework has the potential to lower the barrier of entry for personalizing wearable robots and help further advance their performance.

REFERENCES

[1] P. Kantharaju, H. Jeong, S. Ramadurai, M. Jacobson, H. Jeong, and M. Kim, "Reducing squat physical effort using personalized assistance from an ankle exoskeleton," *IEEE Trans. Neural Syst. Rehabil. Eng.*, vol. 30, pp. 1786–1795, 2022.

[2] M. Jacobson, P. Kantharaju, H. Jeong, J.-K. Ryu, J.-J. Park, H.-J. Chung, and M. Kim, "Foot contact forces can be used to personalize a wearable robot during human walking," *Sci. Rep.*, vol. 12, no. 1, p. 10947, Jun. 2022.

[3] J. Zhang, P. Fiers, K. A. Witte, R. W. Jackson, K. L. Poggensee, C. G. Atkeson, and S. H. Collins, "Human-in-the-loop optimization of exoskeleton assistance during walking," *Science*, vol. 356, no. 6344, pp. 1280–1284, Jun. 2017.

[4] K. A. Witte, P. Fiers, A. L. Sheets-Singer, and S. H. Collins, "Improving the energy economy of human running with powered and unpowered ankle exoskeleton assistance," *Sci. Robot.*, vol. 5, no. 40, Mar. 2020, Art. no. eaay9108.

[5] P. Slade, M. J. Kochenderfer, S. L. Delp, and S. H. Collins, "Personalizing exoskeleton assistance while walking in the real world," *Nature*, vol. 610, no. 7931, pp. 277–282, Oct. 2022.

[6] M. Kim and S. H. Collins, "Once-per-step control of ankle push-off work improves balance in a three-dimensional simulation of bipedal walking," *IEEE Trans. Robot.*, vol. 33, no. 2, pp. 406–418, Apr. 2017.

[7] M. Kim, H. Jeong, P. Kantharaju, D. Yoo, M. Jacobson, D. Shin, C. Han, and J. L. Patton, "Visual guidance can help with the use of a robotic exoskeleton during human walking," *Sci. Rep.*, vol. 12, no. 1, p. 3881, Mar. 2022.

[8] L. N. Awad, P. Kudzia, D. A. Revi, T. D. Ellis, and C. J. Walsh, "Walking faster and farther with a soft robotic exosuit: Implications for post-stroke gait assistance and rehabilitation," *IEEE Open J. Eng. Med. Biol.*, vol. 1, pp. 108–115, 2020.

[9] J. Vaughan-Graham, D. Brooks, L. Rose, G. Nejat, J. Pons, and K. Patterson, "Exoskeleton use in post-stroke gait rehabilitation: A qualitative study of the perspectives of persons post-stroke and physiotherapists," *J. Neuroeng. Rehabil.*, vol. 17, no. 1, p. 123, Sep. 2020.

[10] R. E. Quesada, J. M. Caputo, and S. H. Collins, "Increasing ankle push-off work with a powered prosthesis does not necessarily reduce metabolic rate for transtibial amputees," *J. Biomech.*, vol. 49, no. 14, pp. 3452–3459, Oct. 2016.

[11] C. G. Welker, A. S. Voloshina, V. L. Chiu, and S. H. Collins, "Shortcomings of human-in-the-loop optimization of an ankle-foot prosthesis emulator: A case series," *Roy. Soc. Open Sci.*, vol. 8, no. 5, May 2021, Art. no. 202020.

[12] R. W. Nuckols, K. Z. Takahashi, D. J. Farris, S. Mizrachi, R. Riemer, and G. S. Sawicki, "Mechanics of walking and running up and downhill: A joint-level perspective to guide design of lower-limb exoskeletons," *PLoS One*, vol. 15, no. 8, Aug. 2020, Art. no. e0231996.

[13] N. Stergiou, R. T. Harbourne, and J. T. Cavanaugh, "Optimal movement variability: A new theoretical perspective for neurologic physical therapy," *J. Neurolog. Phys. Therapy*, vol. 30, no. 3, pp. 120–129, Sep. 2006.

[14] P. Antonellis, S. Galle, D. De Clercq, and P. Malcolm, "Altering gait variability with an ankle exoskeleton," *PLoS One*, vol. 13, no. 10, Oct. 2018, Art. no. e0205088.

[15] J. Zhang, C. C. Cheah, and S. H. Collins, "Torque control in legged locomotion," in *Bioinspired Legged Locomotion*. Amsterdam, The Netherlands: Elsevier, 2017, pp. 347–400.

[16] Y. Ding, M. Kim, S. Kuindersma, and C. J. Walsh, "Human-in-the-loop optimization of hip assistance with a soft exosuit during walking," *Sci. Robot.*, vol. 3, no. 15, pp. 1–9, Feb. 2018.

[17] M. Kim, Y. Ding, P. Malcolm, J. Speeckaert, C. J. Siviy, C. J. Walsh, and S. Kuindersma, "Human-in-the-loop Bayesian optimization of wearable device parameters," *PLoS One*, vol. 12, no. 9, Sep. 2017, Art. no. e0184054.

[18] J. R. Koller et al., "'Body-in-the-loop' optimization of assistive robotic devices: A validation study," *Robot., Sci. Syst.*, vol. 2016, pp. 1–10, 2016.

[19] W. Felt, J. C. Selinger, J. M. Donelan, and C. D. Remy, "'Body-in-the-loop': Optimizing device parameters using measures of instantaneous energetic cost," *PLoS One*, vol. 10, no. 8, pp. 1–21, Aug. 2015.

[20] G. M. Bryan, P. W. Franks, S. Song, A. S. Voloshina, R. Reyes, M. P. O'Donovan, K. N. Gregorczyk, and S. H. Collins, "Optimized hip–knee–ankle exoskeleton assistance at a range of walking speeds," *J. Neuroeng. Rehabil.*, vol. 18, p. 152, Mar. 2021.

[21] P. W. Franks, G. M. Bryan, R. Reyes, M. P. O'Donovan, K. N. Gregorczyk, and S. H. Collins, "The effects of incline level on optimized lower-limb exoskeleton assistance," *IEEE Trans. Neural Syst. Rehabil. Eng.*, vol. 30, pp. 2494–2505, 2022.

[22] P. Kantharaju and M. Kim, "Phase-plane based model-free estimation of steady-state metabolic cost," *IEEE Access*, vol. 10, pp. 97642–97650, 2022.

[23] T.-C. Wen, M. Jacobson, X. Zhou, H.-J. Chung, and M. Kim, "The personalization of stiffness for an ankle-foot prosthesis emulator using human-in-the-loop optimization," in *Proc. IEEE/RSJ Int. Conf. Intell. Robots Syst. (IROS)*, Oct. 2020, pp. 3431–3436.

[24] D. M. Blei and M. I. Jordan, "Variational inference for Dirichlet process mixtures," *Bayesian Anal.*, vol. 1, no. 1, pp. 121–143, Mar. 2006.

[25] N. Nasios and A. G. Bors, "Blind source separation using variational expectation-maximization algorithm," in *Proc. Int. Conf. Comput. Anal. Images Patterns*. Cham, Switzerland: Springer, 2003, pp. 442–450.

[26] N. Nasios and A. G. Bors, "Variational learning for Gaussian mixture models," *IEEE Trans. Syst., Man Cybern., B, Cybern.*, vol. 36, no. 4, pp. 849–862, Aug. 2006.

[27] H. Han, W. Wang, F. Zhang, X. Li, J. Chen, J. Han, and J. Zhang, "Selection of muscle-activity-based cost function in human-in-the-loop optimization of multi-gait ankle exoskeleton assistance," *IEEE Trans. Neural Syst. Rehabil. Eng.*, vol. 29, pp. 944–952, 2021.

[28] H. Jeong, P. Haghighat, P. Kantharaju, M. Jacobson, H. Jeong, and M. Kim, "Muscle coordination and recruitment during squat assistance using a robotic ankle–foot exoskeleton," *Sci. Rep.*, vol. 13, no. 1, p. 1363, Jan. 2023.

[29] K. A. Ingraham, E. J. Rouse, and C. D. Remy, "Accelerating the estimation of metabolic cost using signal derivatives: Implications for optimization and evaluation of wearable robots," *IEEE Robot. Autom. Mag.*, vol. 27, no. 1, pp. 32–42, Mar. 2020.

[30] S. Michael, K. S. Graham, and G. M. Davis, "Cardiac autonomic responses during exercise and post-exercise recovery using heart rate variability and systolic time intervals—A review," *Front. Physiol.*, vol. 8, p. 301, 2017.

[31] M. P. Tulppo, T. H. Makikallio, T. E. Takala, T. Seppanen, and H. V. Huikuri, "Quantitative beat-to-beat analysis of heart rate dynamics during exercise," *Amer. J. Physiol.-Heart Circulatory Physiol.*, vol. 271, no. 1, pp. H244–H252, Jul. 1996.

[32] L. Mourot, M. Bouhaddi, S. Perrey, J.-D. Rouillon, and J. Regnard, "Quantitative Poincaré plot analysis of heart rate variability: Effect of endurance training," *Eur. J. Appl. Physiol.*, vol. 91, no. 1, pp. 79–87, Jan. 2004.

[33] F. Shaffer, R. McCraty, and C. L. Zerr, "A healthy heart is not a metronome: An integrative review of the heart's anatomy and heart rate variability," *Front. Psychol.*, vol. 5, p. 1040, Sep. 2014.

[34] A. B. Ciccone, J. A. Siedlik, J. M. Wecht, J. A. Deckert, N. D. Nguyen, and J. P. Weir, "Reminder: RMSSD and SD1 are identical heart rate variability metrics," *Muscle Nerve*, vol. 56, no. 4, pp. 674–678, Oct. 2017.

[35] C. Povea, L. Schmitt, J. Brugniaux, G. Nicolet, J.-P. Richalet, and J.-P. Fouillot, "Effects of intermittent hypoxia on heart rate variability during rest and exercise," *High Altitude Med. Biol.*, vol. 6, no. 3, pp. 215–225, Sep. 2005.

[36] A. S. Leicht, W. H. Sinclair, and W. L. Spinks, "Effect of exercise mode on heart rate variability during steady state exercise," *Eur. J. Appl. Physiol.*, vol. 102, no. 2, pp. 195–204, Nov. 2007.

[37] I. Garcia-Tabar, L. Sánchez-Medina, J. F. Aramendi, M. Ruesta, J. Ibañez, and E. Gorostiaga, "Heart rate variability thresholds predict lactate thresholds in professional world-class road cyclists," *J. Exerc. Physiol. Online*, vol. 16, pp. 38–50, Jan. 2013.

[38] P. Slade, R. Troutman, M. J. Kochenderfer, S. H. Collins, and S. L. Delp, "Rapid energy expenditure estimation for ankle assisted and inclined loaded walking," *J. Neuroeng. Rehabil.*, vol. 16, no. 1, p. 67, Dec. 2019.

[39] J. C. Selinger and J. M. Donelan, "Estimating instantaneous energetic cost during non-steady-state gait," *J. Appl. Physiol.*, vol. 117, no. 11, pp. 1406–1415, Dec. 2014.

[40] M. Kim, H. Lyness, T. Chen, and S. H. Collins, "The effects of prosthesis inversion/eversion stiffness on balance-related variability during level walking: A pilot study," *J. Biomech. Eng.*, vol. 142, no. 9, Sep. 2020, Art. no. 091011.

[41] J. Kim, P. Kantharaju, H. Yi, M. Jacobson, H. Jeong, H. Kim, J. Lee, J. Matthews, N. Zavanelli, H. Kim, H. Jeong, M. Kim, and W.-H. Yeo, "Soft wearable flexible bioelectronics integrated with an ankle-foot exoskeleton for estimation of metabolic costs and physical effort," *npj Flexible Electron.*, vol. 7, no. 1, pp. 1–10, Jan. 2023.

[42] B. J. Whipp, "Dynamics of pulmonary gas exchange," *Circulation*, vol. 76, pp. VI18–VI28, Dec. 1987.

[43] J. M. Brockway, "Derivation of formulae used to calculate energy expenditure in man," *Hum. Nutrition, Clin. Nutrition*, vol. 41, no. 6, pp. 463–471, Nov. 1987.

[44] H. G. Sung, "Gaussian mixture regression and classification," Ph.D Thesis, Dept. Statist., RICE Univ., Houstan, TX, USA, 2004. [Online]. Available: https://scholarship.rice.edu/handle/1911/18710

[45] P. Hamilton, "Open source ECG analysis," in *Proc. Comput. Cardiol.*, Sep. 2002, pp. 101–104.

[46] V. Kalidas and L. Tamil, "Real-time QRS detector using stationary wavelet transform for automated ECG analysis," in *Proc. IEEE 17th Int. Conf. Bioinf. Bioeng. (BIBE)*, Oct. 2017, pp. 457–461.

[47] D. Makowski, T. Pham, Z. J. Lau, J. C. Brammer, F. Lespinasse, H. Pham, C. Schölzel, and S. H. A. Chen, "NeuroKit2: A Python toolbox for neurophysiological signal processing," *Behav. Res. Methods*, vol. 53, no. 4, pp. 1689–1696, Feb. 2021.

[48] H. J. Baek, C.-H. Cho, J. Cho, and J.-M. Woo, "Reliability of ultra-short-term analysis as a surrogate of standard 5-min analysis of heart rate variability," *Telemed. e-Health*, vol. 21, no. 5, pp. 404–414, May 2015.

[49] R. O. Robinson, W. Herzog, and B. M. Nigg, "Use of force platform variables to quantify the effects of chiropractic manipulation on gait symmetry," *J. Manipulative Physiol. Therapeutics*, vol. 10, no. 4, pp. 172–176, Aug. 1987.

[50] J. Snoek, H. Larochelle, and R. P. Adams, "Practical Bayesian optimization of machine learning algorithms," in *Proc. Adv. Neural Inf. Process. Syst.*, vol. 25. Red Hook, NY, USA: Curran Associates, 2012, pp. 1–9.

[51] M. Pelikan, D. E. Goldberg, and E. Cantú-Paz, "BOA: The Bayesian optimization algorithm," in *Proc. Genetic Evol. Comput. Conf.*, 1999, pp. 1–8.

[52] E. Schulz, M. Speekenbrink, and A. Krause, "A tutorial on Gaussian process regression: Modelling, exploring, and exploiting functions," *J. Math. Psychol.*, vol. 85, pp. 1–16, Aug. 2018.

[53] C. K. Williams and C. E. Rasmussen, *Gaussian Processes for Machine Learning*. Cambridge, MA, USA: MIT Press, 2006.

[54] P. I. Frazier, "Bayesian optimization," in *Recent Advances in Optimization and Modeling of Contemporary Problems*. Phoenix, AZ, USA: INFORMS, 2018, pp. 255–278.

[55] M. Balandat, B. Karrer, D. R. Jiang, S. Daulton, B. Letham, A. Gordon Wilson, and E. Bakshy, "BoTorch: A framework for efficient Monte-Carlo Bayesian optimization," 2019, *arXiv:1910.06403*.

[56] R. Benassi, J. Bect, and E. Vazquez, "Bayesian optimization using sequential Monte Carlo," in *Learning and Intelligent Optimization* (Lecture Notes in Computer Science), Y. Hamadi and M. Schoenauer, Eds. Berlin, Germany: Springer, 2012, pp. 339–342.

[57] R. Hanspal, K. Fisher, and R. Nieveen, "Prosthetic socket fit comfort score," *Disab. Rehabil.*, vol. 25, no. 22, pp. 1278–1280, Nov. 2003.

[58] D. J. Farris and G. S. Sawicki, "The mechanics and energetics of human walking and running: A joint level perspective," *J. Roy. Soc. Interface*, vol. 9, no. 66, pp. 110–118, Jan. 2012.

[59] C. A. Zirker, B. C. Bennett, and M. F. Abel, "Changes in kinematics, metabolic cost, and external work during walking with a forward assistive force," *J. Appl. Biomech.*, vol. 29, no. 4, pp. 481–489, Aug. 2013.

[60] M. Kim, C. Liu, J. Kim, S. Lee, A. Meguid, C. J. Walsh, and S. Kuindersma, "Bayesian optimization of soft exosuits using a metabolic estimator stopping process," in *Proc. Int. Conf. Robot. Automat. (ICRA)*, Aug. 2019, pp. 9173–9179.
[61] K. L. Poggensee and S. H. Collins, "How adaptation, training, and customization contribute to benefits from exoskeleton assistance," *Sci. Robot.*, vol. 6, no. 58, Sep. 2021, Art. no. eabf1078.
[62] S. N. Simha, J. D. Wong, J. C. Selinger, S. J. Abram, and J. M. Donelan, "Increasing the gradient of energetic cost does not initiate adaptation in human walking," *J. Neurophysiol.*, vol. 126, no. 2, pp. 440–450, Aug. 2021.
[63] X. Zhou and N. Shroff, "No-regret algorithms for time-varying Bayesian optimization," in *Proc. 55th Annu. Conf. Inf. Sci. Syst. (CISS)*. Baltimore, MD, USA: IEEE, Mar. 2021, pp. 1–6.
[64] M. Jacobson, P. Kantharaju, S. S. Vakacherla, and M. Kim, "A two-degree-of-freedom ankle exoskeleton with control of plantarflexion and inversion-eversion torque," *IEEE/ASME Trans. Mechatronics*, to be published.
[65] M. Kim, M. Jacobson, P. Kantharaju, and H. Jeong, "Robotic ankle exoskeleton for human-in-the-loop design," in *Proc. US-Korea Conf.*, 2021.
[66] I. Sanz-Pena, H. Jeong, and M. Kim, "Personalized wearable ankle robot using modular additive manufacturing design," *IEEE Robot. Automat. Lett.*, vol. 8, no. 8, pp. 4935–4942, Aug. 2023.

PRAKYATH KANTHARAJU (Member, IEEE) received the B.E. degree from Visvesvaraya Technological University, in 2017, and the M.S. degree from the University of Illinois at Chicago, Chicago, IL, USA, in 2019, where he is currently pursuing the Ph.D. degree. His research interest includes human–robot interaction, machine learning, and biomedical signal processing.

SAI SIDDARTH VAKACHERLA received the B.Tech. degree in mechanical engineering from the Indian Institute of Technology, Bhilai, in 2021. He is currently pursuing the M.S. degree with the University of Illinois at Chicago, Chicago, IL, USA. His research interests include wearable robotics and data-driven optimization.

MICHAEL JACOBSON (Member, IEEE) received the B.E. degree from the University of Illinois at Chicago, Chicago, IL, USA, in 2019, where he is currently pursuing the Ph.D. degree. His research interests include wearable robot design, machine learning, and biomedical signal processing.

HYEONGKEUN JEONG (Member, IEEE) received the B.S. degree from Korea University, Seoul, South Korea, in 2016, and the M.S. degree from the University of California at Los Angeles, Los Angeles, CA, USA, in 2019. He is currently pursuing the Ph.D. degree in mechanical and industrial engineering with the University of Illinois at Chicago, Chicago, IL, USA.

MEET NIKUNJ MEVADA received the B.E. degree in mechanical engineering from The Maharaja Sayajirao University of Baroda, in 2019. He was an Automation Engineer with Hariome Spring Industries, Vadodara, for one year. He is currently pursuing the master's degree in mechanical engineering with the University of Illinois at Chicago, Chicago, IL, USA. His research interests include wearable robotics and using deep learning to help control wearable devices in natural environments with systems, such as human activity recognition and walking speed estimation.

XINGYUAN ZHOU (Member, IEEE) received the B.E. degree from the Guangdong University of Technology, Guangzhou, China, in 2020, and the M.S. degree from the University of Illinois at Chicago, Chicago, USA, in 2021. He is currently pursuing the Ph.D. degree with the Department of Electrical and Computer Engineering, New York University, New York, NY, USA. His research interests include human-in-the-loop optimization based on biosignal, physical human–robot interaction, and AI in robotics.

MATTHEW J. MAJOR received the Ph.D. degree. He is currently an Associate Professor of physical medicine and rehabilitation and biomedical engineering with Northwestern University and a Research Health Scientist with the Jesse Brown VA Medical Center, Chicago, IL, USA. He is also a Core Faculty Member of the Northwestern University Prosthetics-Orthotics Center (NUPOC), where he instructs for the master's in Prosthetics and Orthotics Clinical Education Program and directs the NUPOC Prosthetics and Orthotics Rehabilitation Technology Assessment Laboratory (PORTAL). His research interest includes the design and optimization of rehabilitation interventions to enhance mobility of individuals with musculoskeletal and neurological pathology. He serves on the editorial board for the *Journal of Prosthetics and Orthotics*, the Research Committee of The Orthotic and Prosthetic Foundation for Education and Research, and the Scientific Committee of the International Society for Prosthetics and Orthotics. He is an Associate Editor of the *ASME Journal of Biomechanical Engineering*.

MYUNGHEE KIM (Member, IEEE) received the B.S. degree from Hanyang University, Seoul, South Korea, in 2002, the first M.S. degree from the Korea Advanced Institute of Science and Technology, Daejeon, South Korea, in 2004, and the second M.S. degree from the Massachusetts Institute of Technology, Cambridge, MA, USA, in 2006, and the Ph.D. degree from Carnegie Mellon University, Pittsburgh, PA, USA, in 2015.

She was a Postdoctoral Researcher with Harvard University, Cambridge, MA, USA, and a Control Engineer in humanoid robotics with Samsung. She is currently an Assistant Professor in mechanical engineering with the University of Illinois at Chicago, Chicago, IL, USA, where she directs the Rehabilitation Robotics Laboratory and teaches courses on control and robotics.

Dr. Kim was a recipient of the Best Paper Award in the medical devices category at the IEEE Robotics and Automation Society, in 2015, and an Advisor of the Best Poster Award from the U.S.–Korea Conference, in 2019.